Frontiers of Information Technology & Electronic Engineering
www.jzus.zju.edu.cn; engineering.cae.cn; www.springerlink.com
ISSN 2095-9184 (print); ISSN 2095-9230 (online)
E-mail: jzus@zju.edu.cn

# Passivity-based synchronous control of Markov jump systems with actuator saturation*

Liqing WANG[†‡1], Jiaming TANG[†1], Mingkun WANG[1], Feiyu YANG[2]

[1]*School of Mechanical Engineering, Zhejiang Sci-Tech University, Hangzhou 310018, China*

[2]*School of Software Technology, Zhejiang University, Hangzhou 310027, China*

[†]E-mail: liqingwang@zju.edu.cn; 202230503233@mails.zstu.edu.cn

Received Jan. 16, 2025; Revision accepted May 19, 2025; Crosschecked Aug. 28, 2025

**Abstract:** In this article, the robust control problem of discrete-time Markov jump systems (MJSs) with actuator saturation is investigated via the passivity theory. Under the assumption of mode synchronization between the system and the controller, sufficient conditions are established to guarantee the system to be mean-square stable and stochastically passive in the domain of attraction via the saturation-dependent Lyapunov function approach and the linear matrix inequality (LMI) technique. The coupling between the system variables is decoupled, which greatly facilitates the design of the synchronization controller. Moreover, the estimation of the domain of attraction for the considered MJSs is accomplished through the solution of an optimization problem (OP). By degenerating the mode-dependent controller into its mode-independent counterpart, we derive sufficient conditions to ensure system robustness under the mode-independent control strategy, and then systematically summarize these conditions. Finally, the effectiveness of the proposed integrated design methodology is validated through numerical simulations.

**Key words:** Markov jump systems; Synchronous controller; Actuator saturation; Passivity; Linear matrix inequalities

https://doi.org/10.1631/FITEE.2500039 **CLC number:** TP13

## 1 Introduction

Markov jump systems (MJSs), as a specialized category of stochastic hybrid systems in network control architectures, have attracted significant academic attention due to their unique capability of concurrently characterizing both external environmental variations and internal parameter transitions. These distinctive features have led to widespread applications across multiple engineering domains (Costa et al., 2005; Cheng et al., 2020; Chen et al., 2022a, 2023, 2024; Pang et al., 2024; Wang S and Wu, 2024). There exist two fundamental control strategies in MJSs, namely, output feedback control and state feedback control. Specifically, output feedback control relies on the output variables of the system to carry out the design of the controller, and it is constrained by the output matrix (Cheng et al., 2021; Tao and Wu, 2024). In contrast, state feedback control relies on the state variables of the system for the design of the controller. Moreover, based on the synchronization between the modes of the state feedback controller and those of the system, the design methods can be classified into three categories.

1. The mode-independent (MID) control strategy, in which the state feedback gain matrix is fixed and does not change with time (Goncalves et al., 2009; Oliveira et al., 2014; Nie et al., 2024). This strategy can ensure the system robustness in the complete absence of mode information, but it has inherent conservatism.

2. The asynchronous control strategy, in which

‡ Corresponding author

* Project supported by the National Natural Science Foundation of China (No. 62303421) and the Zhejiang Provincial Natural Science Foundation of China (No. LQ23F030018)

ORCID: Liqing WANG, https://orcid.org/0000-0002-0224-3909

the state feedback gain matrix is not fixed and its transition law is inconsistent with the system mode transition (Wu ZG et al., 2014; Wu YY et al., 2021; Wang S et al., 2023). The asynchronous control strategy can enhance system performance in the presence of mode mismatch. However, it introduces additional variable coupling, thereby increasing the complexity of the theoretical framework.

3. The mode-dependent (MD) control method, in which the state feedback gain matrix is also not fixed (Zhao et al., 2012; Bolzern et al., 2014; Feng and Shi, 2017; Zhang et al., 2018; Xu TS et al., 2024). However, different from the asynchronous control strategy, this method uses the assumption of complete synchronization; that is, the transition law of the controller mode is completely consistent with the system mode transition. Without additional variable coupling, it is considered a more efficient and convenient approach.

Actuator saturation is an important cause of system nonlinearity and instability (Hu and Lin, 2001). Owing to the inherent physical limitations of actuator components and other factors, the control output of systems exhibiting actuator saturation is constrained. This limitation will cause system performance degradation and even a system crash. Jiang et al. (2021) investigated an event-triggered $H_\infty$ controller design for discrete-time piecewise-affine systems with actuator saturation. The problem of robust $H_\infty$ control has been studied for MJSs characterized by actuator saturation and incomplete knowledge of transition probabilities (Wang YJ et al., 2012). An asynchronous control strategy ensuring mean-square stability for MJSs with actuator saturation has been introduced in another work (Wang S and Wu, 2022). Therefore, studying MJSs with actuator saturation based on passivity is a novel research direction. The concept of passivity is introduced below:

Passivity, regarded as one of the pivotal performance metrics for system robustness, underpins the stable operation of systems amidst intricate operational conditions and interfering environments. It leverages the inherent properties related to energy absorption, storage, and dissipation within the system, effectively enabling the system to withstand uncertainties and perturbations while maintaining its operational integrity and performance stability. In Wu ZG et al. (2017), the mean-square stability and stochastic passivity of discrete-time MJSs were achieved through a passivity-based asynchronous controller. A state feedback sampled-data controller independent of time was designed to address the problem of passivity-based robust sampled-data control for continuous-time MJSs (Chen et al., 2020). When deception attacks occur in the system, the security-based passivity problem of discrete-time MJSs was resolved through asynchronous control (Xu Y et al., 2023). Passivity is one of the properties studied for the system robustness, and its premise is based on the stability of the system. The system stability criteria and controller design methods proposed in Chen et al. (2022b) and (2023) have provided research ideas for this paper.

Inspired by previous research, this paper focuses on using the theory of stochastic passivity to explore the robust mean-square stability issue for MJSs with actuator saturation. The following are the main contributions of this paper:

1. By adopting the Lyapunov function analysis method, we derive sufficient conditions to ensure that the closed-loop system achieves stochastic mean-square stability and stochastic passivity within the attraction domain.

2. By using the linear matrix inequality (LMI) technique, the coupled variables in the sufficient conditions are decoupled.

3. Through ingenious algebraic manipulations, we transform these conditions into a convex optimization problem based on LMI and accordingly estimate the range of the system's attraction domain.

4. The sufficient conditions are degenerated to the MID control strategy, enabling the system to be mean-square stable and stochastically passive.

**Notations** Throughout this paper, the superscript T denotes the matrix transposition. The symbols $\mathbb{R}^n$ ($\mathbb{R}^f$ and $\mathbb{R}^p$) and $\mathbb{R}^{n\times m}$ ($\mathbb{R}^{n\times n}$, $\mathbb{R}^{p\times n}$, $\mathbb{R}^{p\times m}$, and $\mathbb{R}^{n\times f}$) represent the $n$ ($f$ and $p$)-dimensional Euclidean space and the set of all $n\times m$ ($n\times n$, $p\times n$, $p\times m$, and $n\times f$) real matrices, respectively. For probability space ($\mathit{\Gamma}$, $\mathit{\Theta}$, $\mathit{\Lambda}$), $\mathit{\Gamma}$ represents the sample space, $\mathit{\Theta}$ is the algebra of events, and $\mathit{\Lambda}$ stands for the probability measure defined on $\mathit{\Theta}$. The symbol $\mathcal{E}\{\}$ represents the expectation operator. The notation $\boldsymbol{P}>0$ ($\boldsymbol{P}\geq 0$) means that $\boldsymbol{P}$ is symmetric and positive definite (positive semi-definite), while $\boldsymbol{P}<0$ ($\boldsymbol{P}\leq 0$) means that $\boldsymbol{P}$ is symmetric and negative definite (negative semi-definite). The symbol diag$\{\}$

represents a block diagonal matrix. In symmetric block matrices, we use $*$ as an ellipsis for terms that are induced by symmetry.

## 2 Preliminaries

In the context of a specified probability space $(\Gamma,\ \Theta,\ \Lambda)$, the focus is on the consideration of the following MJSs:

$$\begin{cases} \boldsymbol{x}(k+1)=\boldsymbol{A}(r(k))\boldsymbol{x}(k)+\boldsymbol{B}(r(k))\boldsymbol{\sigma}(\boldsymbol{u}(k)) \\ \qquad\qquad +\boldsymbol{F}(r(k))\boldsymbol{\omega}(k), \\ \boldsymbol{z}(k)=\boldsymbol{C}(r(k))\boldsymbol{x}(k)+\boldsymbol{D}(r(k))\boldsymbol{\sigma}(\boldsymbol{u}(k)). \end{cases} \tag{1}$$

The matrices $\boldsymbol{A}(r(k))\in\mathbb{R}^{n\times n}$, $\boldsymbol{B}(r(k))\in\mathbb{R}^{n\times m}$, $\boldsymbol{C}(r(k))\in\mathbb{R}^{p\times n}$, $\boldsymbol{D}(r(k))\in\mathbb{R}^{p\times m}$, $\boldsymbol{F}(r(k))\in\mathbb{R}^{n\times f}$ represent the system parameters, and $k$ denotes the time. The system state variable is denoted by $\boldsymbol{x}(k)\in\mathbb{R}^n$, while the control input is denoted by $\boldsymbol{u}(k)\in\mathbb{R}^m$. The symbol $\boldsymbol{\omega}(k)\in\mathbb{R}^f$ signifies an external disturbance from the environment, which belongs to the $l_2$ space over the interval $[0,\ \infty)$, and $\boldsymbol{z}(k)\in\mathbb{R}^p$ denotes the controlled output. We define $\boldsymbol{\sigma}(u_v)=\operatorname{sign}(u_v)\min\{1,\ |u_v|\}$, $v=1,2,\cdots,m$. Subsequently, the standard saturation function $\boldsymbol{\sigma}(\boldsymbol{u}(k))$ is presented as follows:

$$\boldsymbol{\sigma}(\boldsymbol{u}(k))=\begin{bmatrix}\boldsymbol{\sigma}(u_1(k)) & \boldsymbol{\sigma}(u_2(k)) & \dots & \boldsymbol{\sigma}(u_m(k))\end{bmatrix}^{\mathrm{T}}.$$

The transition probability matrix (TPM) of the system is expressed as $\boldsymbol{\Pi}$, an $N\times N$ matrix with element of $\pi_{ij}$. The system mode $r(k)$ depends on a homogeneous Markov process $\{r(k),k\geq 0\}$. It is defined as follows:

$$\Pr\{r(k+1)=j|r(k)=i\}=\pi_{ij}, \tag{2}$$

where $i,j\in\mathcal{N}$, $0\leq\pi_{ij}\leq 1$, $\sum_{j=1}^{N}\pi_{ij}=1$, positive integer set $\mathcal{N}=\{1,2,\dots,N\}$, and $N$ is pre-known, referring to the number of modes of the system. The definition of the synchronous controller is given as follows:

$$\boldsymbol{u}(k)=\boldsymbol{K}(r(k))\boldsymbol{x}(k), \tag{3}$$

where $\boldsymbol{K}(r(k))\in\mathbb{R}^{m\times n}$.

To further develop the research in this paper, we introduce some crucial concepts and definitions. They are listed below:

Considering a symmetric polyhedron set $\mathcal{L}(\boldsymbol{H}_i)$, its definition is considered as follows:

$$\mathcal{L}(\boldsymbol{H}_i)=\{\boldsymbol{x}(k)\in\mathbb{R}^n:|\boldsymbol{h}_{iq}\boldsymbol{x}(k)|\leq 1\}. \tag{4}$$

Further, the definition of an ellipsoid set $\Omega(P_{il})$ is given as follows:

$$\Omega(\boldsymbol{P}_{il})=\left\{\boldsymbol{x}(k)\in\mathbb{R}^n:\boldsymbol{x}^{\mathrm{T}}(k)\boldsymbol{P}_{il}\boldsymbol{x}(k)\leq 1\right\}, \tag{5}$$

where matrix $\boldsymbol{P}_{il}\geq 0$, and $\boldsymbol{h}_{iq}$ denotes the $q^{\text{th}}$ row of $\boldsymbol{H}_i$.

**Definition 1** (Liu et al., 2006) Set $\mathcal{D}\subset\mathbb{R}^n$ is considered the domain of attraction of the mean-square scene (DoA-MSS) of MJSs in Eq. (1), if the following inequality is true:

$$\mathcal{E}\left\{\sum_{k=0}^{\infty}\|\boldsymbol{x}(k,x_0,r_0)\|^2|x_0,r_0\right\}<\infty, \tag{6}$$

where $x_0$ is the initial state of the system, $r_0$ is the initial mode of the system, and $\boldsymbol{x}(0)$ belongs to set $\mathcal{D}$.

**Definition 2** The MJSs in Eq. (1) are said to be stochastically passive, if there exists a scalar $\gamma>0$ such that the following inequality

$$2\sum_{s=0}^{k_0}\mathcal{E}\{\boldsymbol{z}^{\mathrm{T}}(s)\boldsymbol{\omega}(s)\}\geq-\gamma\sum_{s=0}^{k_0}||\boldsymbol{\omega}(s)||^2 \tag{7}$$

is true under the zero initial condition, where $k_0\geq 0$ denotes the random time from 0 to $k$.

**Lemma 1** (Hu and Lin, 2001) If $\boldsymbol{x}(k)\in\mathcal{L}(\boldsymbol{H}_i)$, the standard actuator saturation function $\boldsymbol{\sigma}(\boldsymbol{u}(k))=\boldsymbol{\sigma}(\boldsymbol{K}_i\boldsymbol{x}(k))$ is further defined as follows:

$$\boldsymbol{\sigma}(\boldsymbol{K}_i\boldsymbol{x}(k))=\sum_{l=1}^{2^m}\eta_l(k)(\boldsymbol{M}_l\boldsymbol{K}_i+\boldsymbol{M}_l^-\boldsymbol{H}_i)\boldsymbol{x}(k). \tag{8}$$

The variables $\eta_l(k)$ satisfy the conditions $0\leq\eta_l(k)\leq 1$ and $\sum_{l=1}^{2^m}\eta_l(k)=1$. The matrices $\boldsymbol{K}_i$ and $\boldsymbol{H}_i$ are control gain matrices. The diagonal matrix $\boldsymbol{M}_l$ belongs to $\mathbb{R}^{m\times m}$ and has diagonal elements that are either 1 or 0. Matrix $\boldsymbol{M}_l^-$ is defined as $\boldsymbol{M}_l^-=\boldsymbol{I}-\boldsymbol{M}_l$, where $\boldsymbol{I}$ is the identity matrix.

**Lemma 2** (Cao et al., 2002) For matrices $\boldsymbol{P}_i\in\mathbb{R}^{m\times m}>0$, $\boldsymbol{\phi}_i\in\mathbb{R}^{m\times m}$, and $i\in\mathcal{M}$, positive integer set $\mathcal{M}=\{1,2,\dots,M\}$ ($M$ represents the modal number of the controller), if $\sum_{i=1}^{M}\alpha_i=1, 0\leq\alpha_i\leq 1$, then the following inequality is true:

$$\sum_{i=1}^{M}\alpha_i\boldsymbol{\phi}_i^{\mathrm{T}}\boldsymbol{P}_i\left(\sum_{i=1}^{M}\alpha_i\boldsymbol{\phi}_i\right)\leq\sum_{i=1}^{M}\alpha_i\boldsymbol{\phi}_i^{\mathrm{T}}\boldsymbol{P}_i\boldsymbol{\phi}_i. \tag{9}$$

## 3 Main results

In this section, some sufficient conditions for ensuring the mean-square stability and stochastic passivity of MJSs are given, using saturation-dependent Lyapunov functions and LMI techniques.

**Theorem 1** If there exist $\boldsymbol{P}_{il} > 0$ and scalar $\gamma > 0$ satisfying expressions (10)–(12):

$$\tilde{\boldsymbol{A}}_{il}^{\mathrm{T}} - \tilde{\boldsymbol{B}}_{il}^{\mathrm{T}}\tilde{\boldsymbol{F}}_i^{-1}\tilde{\boldsymbol{B}}_{il} - \boldsymbol{P}_{il} < 0, \tag{10}$$

$$\tilde{\boldsymbol{F}}_i \le 0, \tag{11}$$

$$\Omega(\boldsymbol{P}_{il}) \subset \mathcal{L}(\boldsymbol{H}_i), \tag{12}$$

the MJSs in Eq. (1) are mean-square stable and stochastically passive. Additionally, the set $\bigcap_{i=1}^{N}\bigcap_{l=1}^{2^m}\Omega(\boldsymbol{P}_{il})$ is referred to as the estimation of the DoA-MSS, where

$$\begin{aligned}
\tilde{\boldsymbol{A}}_{il} &= \boldsymbol{A}_{il}^{\mathrm{T}}\sum_{j=1}^{N}\boldsymbol{\pi}_{ij}\boldsymbol{P}_{jt}\boldsymbol{A}_{il},\\
\tilde{\boldsymbol{B}}_{il}^{\mathrm{T}} &= \boldsymbol{A}_{il}^{\mathrm{T}}\sum_{j=1}^{N}\boldsymbol{\pi}_{ij}\boldsymbol{P}_{jt}\boldsymbol{F}_i - \boldsymbol{C}_{il}^{\mathrm{T}},\\
\tilde{\boldsymbol{F}}_i &= \boldsymbol{F}_i^{\mathrm{T}}\sum_{j=1}^{N}\boldsymbol{\pi}_{ij}\boldsymbol{P}_{jt}\boldsymbol{F}_i - \gamma\boldsymbol{I},\\
\boldsymbol{A}_{il} &= \boldsymbol{A}_i + \boldsymbol{B}_i(\boldsymbol{M}_l\boldsymbol{K}_i + \boldsymbol{M}_l^{-}\boldsymbol{H}_i),\\
\boldsymbol{C}_{il} &= \boldsymbol{C}_i + \boldsymbol{D}_i(\boldsymbol{M}_l\boldsymbol{K}_i + \boldsymbol{M}_l^{-}\boldsymbol{H}_i).
\end{aligned}$$

**Proof** It is assumed that $\boldsymbol{x}(0)$ belongs to the set $\bigcap_{i=1}^{N}\bigcap_{l=1}^{2^m}\Omega(\boldsymbol{P}_{il})$. According to expression (12), it can be deduced that $\boldsymbol{x}(0)$ is within $\mathcal{L}(\boldsymbol{H}_i)$. To fully leverage the available information, a stochastic Lyapunov function that depends on both saturation and system mode is introduced as follows:

$$\boldsymbol{\mathcal{V}}(k) = \boldsymbol{x}^{\mathrm{T}}(k)\left(\sum_{l=1}^{2^m}\eta_l(k)\boldsymbol{P}_{il}\right)\boldsymbol{x}(k). \tag{13}$$

Before further derivation, some important parameters are calculated as below:

$$\begin{aligned}
\boldsymbol{x}(k+1) &= \boldsymbol{A}(r(k))\boldsymbol{x}(k) + \boldsymbol{F}(r(k))\boldsymbol{\omega}(k) + \boldsymbol{B}(r(k))\\
&\quad\cdot\sum_{l=1}^{2^m}\eta_l(k)(\boldsymbol{M}_l\boldsymbol{K}_i + \boldsymbol{M}_l^{-}\boldsymbol{H}_i)\boldsymbol{x}(k)\\
&= \sum_{l=1}^{2^m}\eta_l(k)\boldsymbol{A}_{il}\boldsymbol{x}(k) + \boldsymbol{F}_i\boldsymbol{\omega}(k),
\end{aligned} \tag{14}$$

$$\begin{aligned}
\boldsymbol{z}(k) &= \Bigg(\boldsymbol{C}(r(k)) + \boldsymbol{D}(r(k))\sum_{l=1}^{2^m}\eta_l(k)\\
&\quad\cdot(\boldsymbol{M}_l\boldsymbol{K}_i + \boldsymbol{M}_l^{-}\boldsymbol{H}_i)\Bigg)\boldsymbol{x}(k)\\
&= \sum_{l=1}^{2^m}\eta_l(k)\boldsymbol{C}_{il}\boldsymbol{x}(k).
\end{aligned} \tag{15}$$

For simplicity, the symbol $\boldsymbol{A}(r(k))$ is abbreviated to $\boldsymbol{A}_i$, and other system parameters are simplified in the same manner. Combining Eqs. (13) and (14) and Lemma 2, the following definitions can be obtained:

$$\begin{aligned}
&\mathcal{E}\{\boldsymbol{\mathcal{V}}(\boldsymbol{x}(k+1), \theta(k+1)=j|\boldsymbol{x}(k), \theta(k)=i)\}\\
&= \boldsymbol{x}^{\mathrm{T}}(k+1)\sum_{t=1}^{2^m}\eta_t(k+1)\sum_{j=1}^{N}\boldsymbol{\pi}_{ij}\boldsymbol{P}_{jt}\boldsymbol{x}(k+1)\\
&= \sum_{l=1}^{2^m}\eta_l(k)\begin{bmatrix}\boldsymbol{x}(k)\\ \boldsymbol{\omega}(k)\end{bmatrix}^{\mathrm{T}}\begin{bmatrix}\boldsymbol{A}_{il}^{\mathrm{T}}\\ \boldsymbol{F}_i^{\mathrm{T}}\end{bmatrix}\sum_{t=1}^{2^m}\eta_t(k+1)\\
&\quad\cdot\sum_{j=1}^{N}\boldsymbol{\pi}_{ij}\boldsymbol{P}_{jt}\sum_{l=1}^{2^m}\eta_l(k)\begin{bmatrix}\boldsymbol{A}_{il}^{\mathrm{T}}\\ \boldsymbol{F}_i^{\mathrm{T}}\end{bmatrix}^{\mathrm{T}}\begin{bmatrix}\boldsymbol{x}(k)\\ \boldsymbol{\omega}(k)\end{bmatrix}\\
&\le \sum_{t=1}^{2^m}\eta_t(k+1)\sum_{l=1}^{2^m}\eta_l(k)\begin{bmatrix}\boldsymbol{x}(k)\\ \boldsymbol{\omega}(k)\end{bmatrix}^{\mathrm{T}}\begin{bmatrix}\boldsymbol{A}_{il}^{\mathrm{T}}\\ \boldsymbol{F}_i^{\mathrm{T}}\end{bmatrix}\\
&\quad\cdot\sum_{j=1}^{N}\boldsymbol{\pi}_{ij}\boldsymbol{P}_{jt}\begin{bmatrix}\boldsymbol{A}_{il}^{\mathrm{T}}\\ \boldsymbol{F}_i^{\mathrm{T}}\end{bmatrix}^{\mathrm{T}}\begin{bmatrix}\boldsymbol{x}(k)\\ \boldsymbol{\omega}(k)\end{bmatrix},
\end{aligned} \tag{16}$$

$$\begin{aligned}
&\mathcal{E}\{\Delta\boldsymbol{\mathcal{V}}(k)\}\\
&= \boldsymbol{\mathcal{V}}(\boldsymbol{x}(k+1), \theta(k+1)=j|\boldsymbol{x}(k), \theta(k)=i) - \boldsymbol{\mathcal{V}}(k)\\
&\le \sum_{t=1}^{2^m}\eta_t(k+1)\sum_{l=1}^{2^m}\eta_l(k)\begin{bmatrix}\boldsymbol{x}(k)\\ \boldsymbol{\omega}(k)\end{bmatrix}^{\mathrm{T}}\begin{bmatrix}\boldsymbol{A}_{il}^{\mathrm{T}}\\ \boldsymbol{F}_i^{\mathrm{T}}\end{bmatrix}\sum_{j=1}^{N}\boldsymbol{\pi}_{ij}\boldsymbol{P}_{jt}\\
&\quad\cdot\begin{bmatrix}\boldsymbol{A}_{il}^{\mathrm{T}}\\ \boldsymbol{F}_i^{\mathrm{T}}\end{bmatrix}^{\mathrm{T}}\begin{bmatrix}\boldsymbol{x}(k)\\ \boldsymbol{\omega}(k)\end{bmatrix} - \boldsymbol{x}^{\mathrm{T}}(k)\sum_{l=1}^{2^m}\eta_l(k)\boldsymbol{P}_{il}\boldsymbol{x}(k).
\end{aligned} \tag{17}$$

If $\boldsymbol{\omega}(k) \equiv 0$, then $\mathcal{E}\{\Delta\boldsymbol{\mathcal{V}}(k)\} < 0$ can be made sure by the following inequality:

$$\boldsymbol{A}_{il}^{\mathrm{T}}\sum_{j=1}^{N}\boldsymbol{\pi}_{ij}\boldsymbol{P}_{jt}\boldsymbol{A}_{il} - \boldsymbol{P}_{il} \le 0. \tag{18}$$

Noting $\sum_{t=1}^{2^m}\eta_t(k+1) = 1$ and $\sum_{l=1}^{2^m}\eta_l(k) = 1$, we can easily obtain expression (18) with condition in Eq. (10). Similar to previous research (Wang S and Wu, 2022), the mean-square stability of the MJSs in Eq. (1) can be satisfied via $\mathcal{E}\{\Delta\boldsymbol{\mathcal{V}}(k)\} < 0$ and Definition 1.

Under the zero initial condition, the definition of $\mathcal{J}$ is considered as follows:

$$\begin{aligned}\mathcal{J} &\triangleq \sum_{s=0}^{k_0}\mathcal{E}\{-2\boldsymbol{z}^{\mathrm{T}}(s)\boldsymbol{\omega}(s)-\gamma\boldsymbol{\omega}^{\mathrm{T}}(s)\boldsymbol{\omega}(s)\}\\ &\leq \sum_{s=0}^{k_0}\mathcal{E}\{-2\boldsymbol{z}^{\mathrm{T}}(s)\boldsymbol{\omega}(s)-\gamma\boldsymbol{\omega}^{\mathrm{T}}(s)\boldsymbol{\omega}(s)+\Delta\boldsymbol{\mathcal{V}}(s)\}\\ &\leq \sum_{s=0}^{k_0}\left(\sum_{t=1}^{2^m}\eta_t(s+1)\sum_{l=1}^{2^m}\eta_l(s)\begin{bmatrix}\boldsymbol{x}(s)\\ \boldsymbol{\omega}(s)\end{bmatrix}^{\mathrm{T}}\left(\begin{bmatrix}\boldsymbol{A}_{il}^{\mathrm{T}}\\ \boldsymbol{F}_i^{\mathrm{T}}\end{bmatrix}\right.\right.\\ &\cdot\left.\sum_{j=1}^{N}\boldsymbol{\pi}_{ij}\boldsymbol{P}_{jt}\begin{bmatrix}\boldsymbol{A}_{il}^{\mathrm{T}}\\ \boldsymbol{F}_i^{\mathrm{T}}\end{bmatrix}^{\mathrm{T}}-\begin{bmatrix}\boldsymbol{0} & \boldsymbol{0}\\ \boldsymbol{0} & \gamma\boldsymbol{I}\end{bmatrix}\right)\begin{bmatrix}\boldsymbol{x}(s)\\ \boldsymbol{\omega}(s)\end{bmatrix}\\ &\quad\left.-2\boldsymbol{x}^{\mathrm{T}}(s)\boldsymbol{C}_{il}^{\mathrm{T}}\boldsymbol{\omega}(s)-\boldsymbol{x}^{\mathrm{T}}(s)\sum_{l=1}^{2^m}\eta_l(s)\boldsymbol{P}_{il}\boldsymbol{x}(s)\right)\\ &= \sum_{s=0}^{k_0}\sum_{t=1}^{2^m}\eta_t(s+1)\sum_{l=1}^{2^m}\eta_l(s)\begin{bmatrix}\boldsymbol{x}(s)\\ \boldsymbol{\omega}(s)\end{bmatrix}^{\mathrm{T}}\boldsymbol{\Theta}_{il}\begin{bmatrix}\boldsymbol{x}(s)\\ \boldsymbol{\omega}(s)\end{bmatrix}\\ &\quad-\boldsymbol{x}^{\mathrm{T}}(s)\sum_{l=1}^{2^m}\eta_l(s)\boldsymbol{P}_{il}\boldsymbol{x}(s),\end{aligned}\tag{19}$$

where

$$\boldsymbol{\Theta}_{il}=\begin{bmatrix}\tilde{\boldsymbol{A}}_{il}^{\mathrm{T}} & \tilde{\boldsymbol{B}}_{il}^{\mathrm{T}}\\ * & \tilde{\boldsymbol{F}}_i^{\mathrm{T}}\end{bmatrix}.$$

Via expression (11), we can obtain

$$\begin{bmatrix}\tilde{\boldsymbol{B}}_{il}^{\mathrm{T}}\tilde{\boldsymbol{F}}_i^{-1}\tilde{\boldsymbol{B}}_{il} & \tilde{\boldsymbol{B}}_{il}^{\mathrm{T}}\\ * & \tilde{\boldsymbol{F}}_i^{\mathrm{T}}\end{bmatrix}\leq 0,$$

and we can further obtain the following:

$$\boldsymbol{\Theta}_{il}\leq\begin{bmatrix}\tilde{\boldsymbol{A}}_{il}^{\mathrm{T}}-\tilde{\boldsymbol{B}}_{il}^{\mathrm{T}}\tilde{\boldsymbol{F}}_i^{-1}\tilde{\boldsymbol{B}}_{il} & \boldsymbol{0}\\ * & \boldsymbol{0}\end{bmatrix}.\tag{20}$$

Combining expressions (19) and (20), $\mathcal{J} < 0$ can be obtained under the following condition:

$$\begin{aligned}&\sum_{t=1}^{2^m}\eta_t(k+1)\sum_{l=1}^{2^m}\eta_l(k)\boldsymbol{x}^{\mathrm{T}}(k)(\tilde{\boldsymbol{A}}_{il}^{\mathrm{T}}\\ &-\tilde{\boldsymbol{B}}_{il}^{\mathrm{T}}\tilde{\boldsymbol{F}}_i^{-1}\tilde{\boldsymbol{B}}_{il}-\boldsymbol{P}_{il})\boldsymbol{x}(k)<0.\end{aligned}\tag{21}$$

Now, it is easy to see that condition (21) is equal to expression (10). It is guaranteed by Theorem 1 that the MJSs in Eq. (1) are mean-square stable and stochastically passive. The proof is completed.

**Theorem 2** If there exist $\bar{\boldsymbol{P}}_{ij} > 0$, $\bar{\boldsymbol{R}}_{ij} > 0$, $\boldsymbol{G}_i > 0$, and scalar $\gamma > 0$ satisfying

$$\begin{bmatrix}\bar{\boldsymbol{R}}_{il}-\boldsymbol{G}_i^{\mathrm{T}}-\boldsymbol{G}_i & \boldsymbol{\mathcal{C}}_{il}^{\mathrm{T}} & \hat{\boldsymbol{\mathcal{A}}}_{il}^{\mathrm{T}}\\ * & -\gamma\boldsymbol{I} & \hat{\boldsymbol{\mathcal{F}}}_i^{\mathrm{T}}\\ * & * & \bar{\boldsymbol{\mathcal{P}}}_{it}\end{bmatrix}<0,\tag{22}$$

$$\begin{bmatrix}-\bar{\boldsymbol{P}}_{il} & \bar{\boldsymbol{P}}_{il}^{\mathrm{T}}\\ * & -\bar{\boldsymbol{R}}_{il}\end{bmatrix}<0,\tag{23}$$

$$\begin{bmatrix}\bar{\boldsymbol{P}}_{il}-\boldsymbol{G}_i^{\mathrm{T}}-\boldsymbol{G}_i & \boldsymbol{y}_{iq}^{\mathrm{T}}\\ * & -1\end{bmatrix}\leq 0,\tag{24}$$

the MJSs in Eq. (1) are mean-square stable and stochastically passive. Here, $\boldsymbol{y}_{iq}$ denotes the $q^{\text{th}}$ row of $\boldsymbol{\mathcal{Y}}_i$. The set $\bigcap_{i=1}^{N}\bigcap_{l=1}^{2^m}\Omega(\boldsymbol{P}_{il})$ is referred to as the estimation of DoA-MSS, where

$$\begin{aligned}&\hat{\boldsymbol{\mathcal{A}}}_{il}^{\mathrm{T}}=\begin{bmatrix}\boldsymbol{\mathcal{A}}_{il}^{\mathrm{T}} & \boldsymbol{\mathcal{A}}_{il}^{\mathrm{T}} & \ldots & \boldsymbol{\mathcal{A}}_{il}^{\mathrm{T}}\end{bmatrix},\\ &\hat{\boldsymbol{\mathcal{F}}}_i^{\mathrm{T}}=\begin{bmatrix}\boldsymbol{F}_i^{\mathrm{T}} & \boldsymbol{F}_i^{\mathrm{T}} & \ldots & \boldsymbol{F}_i^{\mathrm{T}}\end{bmatrix},\\ &\bar{\boldsymbol{\mathcal{P}}}_{it}=-\mathrm{diag}\left\{\boldsymbol{\pi}_{i1}\bar{\boldsymbol{P}}_{1t} \quad \boldsymbol{\pi}_{i2}\bar{\boldsymbol{P}}_{2t} \quad \ldots \quad \boldsymbol{\pi}_{iN}\bar{\boldsymbol{P}}_{Nt}\right\},\\ &\bar{\boldsymbol{P}}_{il}=\boldsymbol{P}_{il}^{-1},\ \bar{\boldsymbol{R}}_{il}=\boldsymbol{R}_{il}^{-1},\\ &\boldsymbol{\mathcal{A}}_{il}^{\mathrm{T}}=\boldsymbol{G}_i^{\mathrm{T}}\boldsymbol{A}_i^{\mathrm{T}}+\boldsymbol{\mathcal{X}}_i^{\mathrm{T}}\boldsymbol{M}_l^{\mathrm{T}}\boldsymbol{B}_i^{\mathrm{T}}+\boldsymbol{\mathcal{Y}}_i^{\mathrm{T}}(\boldsymbol{M}_l^{-})^{\mathrm{T}}\boldsymbol{B}_i^{\mathrm{T}},\\ &\boldsymbol{\mathcal{C}}_{il}^{\mathrm{T}}=-\boldsymbol{G}_i^{\mathrm{T}}\boldsymbol{C}_i^{\mathrm{T}}-\boldsymbol{\mathcal{X}}_i^{\mathrm{T}}\boldsymbol{M}_l^{\mathrm{T}}\boldsymbol{D}_i^{\mathrm{T}}-\boldsymbol{\mathcal{Y}}_i^{\mathrm{T}}(\boldsymbol{M}_l^{-})^{\mathrm{T}}\boldsymbol{D}_i^{\mathrm{T}},\\ &\boldsymbol{\mathcal{X}}_i=\boldsymbol{K}_i\boldsymbol{G}_i,\ \boldsymbol{\mathcal{Y}}_i=\boldsymbol{H}_i\boldsymbol{G}_i.\end{aligned}$$

**Proof** Based on Theorem 1, we can obtain the following condition:

$$\boldsymbol{A}_{il}^{\mathrm{T}}\sum_{j=1}^{N}\boldsymbol{\pi}_{ij}\boldsymbol{P}_{jt}\boldsymbol{A}_{il}-\tilde{\boldsymbol{B}}_{il}^{\mathrm{T}}\tilde{\boldsymbol{F}}_i^{-1}\tilde{\boldsymbol{B}}_{il}-\boldsymbol{P}_{il}+\epsilon\boldsymbol{I}<0,\ \epsilon>0.\tag{25}$$

Noting scalar $\epsilon > 0$, $\boldsymbol{R}_{il}$ is further considered as

$$\boldsymbol{R}_{il}\triangleq\boldsymbol{A}_{il}^{\mathrm{T}}\sum_{j=1}^{N}\boldsymbol{\pi}_{ij}\boldsymbol{P}_{jt}\boldsymbol{A}_{il}-\tilde{\boldsymbol{B}}_{il}^{\mathrm{T}}\tilde{\boldsymbol{F}}_i^{-1}\tilde{\boldsymbol{B}}_{il}+\epsilon\boldsymbol{I}.$$

Condition (23) (i.e., $\boldsymbol{R}_{il}-\boldsymbol{P}_{il}<0$) is used to ensure that $\epsilon$ exists. Then, inequality (26) can be given:

$$-\boldsymbol{R}_{il}+\boldsymbol{A}_{il}^{\mathrm{T}}\sum_{j=1}^{N}\boldsymbol{\pi}_{ij}\boldsymbol{P}_{jt}\boldsymbol{A}_{il}-\tilde{\boldsymbol{B}}_{il}^{\mathrm{T}}\tilde{\boldsymbol{F}}_i^{-1}\tilde{\boldsymbol{B}}_{il}<0.\tag{26}$$

Further, the proposition that inequalities (26) and (27) are equivalent can be proven using the Schur complement:

$$\begin{bmatrix}-\boldsymbol{R}_{il} & -\boldsymbol{C}_{il}^{\mathrm{T}} & \begin{bmatrix}\boldsymbol{A}_{il}^{\mathrm{T}} & \boldsymbol{A}_{il}^{\mathrm{T}} & \ldots & \boldsymbol{A}_{il}^{\mathrm{T}}\end{bmatrix}\\ * & -\gamma\boldsymbol{I} & \begin{bmatrix}\boldsymbol{F}_i^{\mathrm{T}} & \boldsymbol{F}_i^{\mathrm{T}} & \ldots & \boldsymbol{F}_i^{\mathrm{T}}\end{bmatrix}\\ * & * & \bar{\boldsymbol{\mathcal{P}}}_{il}\end{bmatrix}<0.\tag{27}$$

Letting the auxiliary matrix diag$\{\boldsymbol{G}_i \quad \boldsymbol{I} \quad \boldsymbol{I}\}$ and $\boldsymbol{G}_i$ be the undetermined matrix variable pre- and post-multiplying the inequality (27) by matrix diag$\{\boldsymbol{G}_i \quad \boldsymbol{I} \quad \boldsymbol{I}\}$ and its transpose, we can obtain

$$\begin{bmatrix} -\boldsymbol{G}_i^{\mathrm{T}}\boldsymbol{R}_{il}\boldsymbol{G}_i & -\boldsymbol{G}_i^{\mathrm{T}}\boldsymbol{C}_{il}^{\mathrm{T}} & \hat{\boldsymbol{\mathcal{A}}}_{il}^{\mathrm{T}} \\ * & -\gamma\boldsymbol{I} & \hat{\boldsymbol{\mathcal{F}}}_i^{\mathrm{T}} \\ * & * & \bar{\boldsymbol{\mathcal{P}}}_{il} \end{bmatrix} < 0. \tag{28}$$

According to $-\boldsymbol{G}_i^{\mathrm{T}}\boldsymbol{R}_{il}\boldsymbol{G}_i \le \bar{\boldsymbol{R}}_{il} - \boldsymbol{G}_i^{\mathrm{T}} - \boldsymbol{G}_i$, expression (22) is obtained.

According to the definitions of the symmetric polyhedron set $\mathcal{L}(\boldsymbol{H}_i)$ and the ellipsoid set $\Omega(\boldsymbol{P}_{il})$, expression (29) can be satisfied via expression (12):

$$|\boldsymbol{h}_{iq}\boldsymbol{x}(k)| \le 1, \quad \forall \boldsymbol{x}(k) \in \bigcap_{i=1}^{N}\bigcap_{l=1}^{2^m} \Omega\left(\boldsymbol{P}_{il}\right). \tag{29}$$

Furthermore, we have

$$\boldsymbol{h}_{iq}^{\mathrm{T}}\boldsymbol{h}_{iq} - \boldsymbol{P}_{il} \le 0. \tag{30}$$

According to the Schur complement theorem, inequality (30) is equivalent to

$$\begin{bmatrix} -\boldsymbol{P}_{il} & \boldsymbol{h}_{iq}^{\mathrm{T}} \\ * & -1 \end{bmatrix} \le 0. \tag{31}$$

By means of congruent transformation via matrix diag$\{\boldsymbol{G}_i \quad 1\}$ and $-\boldsymbol{G}_i^{\mathrm{T}}\boldsymbol{P}_{il}\boldsymbol{G}_i \le \bar{\boldsymbol{P}}_{il} - \boldsymbol{G}_i^{\mathrm{T}} - \boldsymbol{G}_i$, if inequality (31) holds, we have

$$\begin{bmatrix} -\boldsymbol{G}_i^{\mathrm{T}}\boldsymbol{P}_{il}\boldsymbol{G}_i & \boldsymbol{G}_i^{\mathrm{T}}\boldsymbol{h}_{iq}^{\mathrm{T}} \\ * & -1 \end{bmatrix} \le \begin{bmatrix} \bar{\boldsymbol{P}}_{il} - \boldsymbol{G}_i^{\mathrm{T}} - \boldsymbol{G}_i & \boldsymbol{y}_{iq}^{\mathrm{T}} \\ * & -1 \end{bmatrix} \le 0. \tag{32}$$

The proof is completed.

**Remark 1** The problem of LMI-coupled variables is overcome by introducing $\boldsymbol{G}_i$ and by means of matrix congruence transformation. Moreover, it can be judged using Theorem 2 that $\boldsymbol{x}(0)$ is in the DoA-MSS. To intuitively ascertain whether $\boldsymbol{x}(0)$ is encompassed within the DoA-MSS, the optimal control problem is introduced:

OP1:

$$\sup \tau$$

$$\bar{\boldsymbol{P}}_{il} > 0,\ \bar{\boldsymbol{R}}_{il} > 0,\ \boldsymbol{G}_i > 0,\ \boldsymbol{\mathcal{X}}_i > 0,\ \boldsymbol{\mathcal{Y}}_i > 0$$

$$\text{s.t. (a) } \tau\boldsymbol{x}(0) = \bigcap_{i=1}^{N}\bigcap_{l=1}^{2^m} \Omega(\boldsymbol{P}_{il}),$$
$$\text{(b) LMIs (22)–(24).}$$

Combining the definition of $\Omega(\boldsymbol{P}_{il})$, condition $(a)$ is equivalent to the expression $\tau^2\boldsymbol{x}^{\mathrm{T}}(0)\boldsymbol{P}_{il}\boldsymbol{x}(0) \le 1$. Furthermore, expression (33) can be obtained via the Schur complement:

$$\begin{bmatrix} -\rho & \boldsymbol{x}^{\mathrm{T}}(0) \\ * & -\bar{\boldsymbol{P}}_{il} \end{bmatrix} \le 0. \tag{33}$$

Here, the symbol $\rho = \tau^{-2}$.

Therefore, OP2 can be given as follows:

OP2:

$$\inf \rho$$

$$\bar{\boldsymbol{P}}_{il} > 0,\ \bar{\boldsymbol{R}}_{il} > 0,\ \boldsymbol{G}_i > 0,\ \boldsymbol{\mathcal{X}}_i > 0,\ \boldsymbol{\mathcal{Y}}_i > 0$$

$$\text{s.t. (a) } \begin{bmatrix} -\rho & \boldsymbol{x}^{\mathrm{T}}(0) \\ * & -\bar{\boldsymbol{P}}_{il} \end{bmatrix} \le 0,$$
$$\text{(b) LMIs (22)–(24).}$$

It means that $\boldsymbol{x}(0)$ is in the DoA-MSS, if the optimal value $\rho_{\min} < 1$. Moreover, the smaller value of $\rho_{\min}$ means that the DoA-MSS is closer to the real one. Subsequently, OP2 is applied within the simulation.

In practical engineering projects, real-time acquisition of internal mode information becomes highly costly due to time-delay phenomena caused by the physical characteristics of sensor components and limited network channel resources. The MID control strategy is a classical approach to cope with asynchrony between the system and the controller (Goncalves et al., 2009; Oliveira et al., 2014; Nie et al., 2024). The corollary in Section 3.1 gives the conditions when the controller mode is totally unavailable.

**Remark 2** The MJSs in Eq. (1) are mean-square stable and stochastically passive, and the set $\bigcap_{i=1}^{N}\bigcap_{l=1}^{2^m}\Omega(\boldsymbol{P}_{il})$ is called the estimation of the DoA-MSS, if there exist $\bar{\boldsymbol{P}}_{ij} > 0$, $\bar{\boldsymbol{R}}_{ij} > 0$, $\boldsymbol{G}_i > 0$, and scalar $\gamma > 0$ satisfying expressions (23) and (24) and

$$\begin{bmatrix} \bar{\boldsymbol{R}}_{il} - \boldsymbol{G}_i^{\mathrm{T}} - \boldsymbol{G}_i & \hat{\boldsymbol{\Psi}}_{il}^{\mathrm{T}} & \hat{\boldsymbol{\Xi}}_{il}^{\mathrm{T}} \\ * & -\gamma\boldsymbol{I} & \hat{\boldsymbol{\mathcal{F}}}_i^{\mathrm{T}} \\ * & * & \bar{\boldsymbol{\mathcal{P}}}_{it} \end{bmatrix} < 0, \tag{34}$$

where

$$\hat{\boldsymbol{\Xi}}_{il}^{\mathrm{T}} = \begin{bmatrix} \boldsymbol{\Xi}_{il}^{\mathrm{T}} & \boldsymbol{\Xi}_{il}^{\mathrm{T}} & \dots & \boldsymbol{\Xi}_{il}^{\mathrm{T}} \end{bmatrix},$$
$$\hat{\boldsymbol{\mathcal{F}}}_{i}^{\mathrm{T}} = \begin{bmatrix} \boldsymbol{F}_{i}^{\mathrm{T}} & \boldsymbol{F}_{i}^{\mathrm{T}} & \dots & \boldsymbol{F}_{i}^{\mathrm{T}} \end{bmatrix},$$
$$\boldsymbol{\Xi}_{il}^{\mathrm{T}} = \boldsymbol{G}_i^{\mathrm{T}}\boldsymbol{A}_i^{\mathrm{T}} + \hat{\boldsymbol{\mathcal{X}}}_i^{\mathrm{T}}\boldsymbol{M}_l^{\mathrm{T}}\boldsymbol{B}_i^{\mathrm{T}} + \hat{\boldsymbol{\mathcal{Y}}}_i^{\mathrm{T}}(\boldsymbol{M}_l^{-})^{\mathrm{T}}\boldsymbol{B}_i^{\mathrm{T}},$$
$$\hat{\boldsymbol{\Psi}}_{il}^{\mathrm{T}} = -\boldsymbol{G}_i^{\mathrm{T}}\boldsymbol{C}_i^{\mathrm{T}} - \hat{\boldsymbol{\mathcal{X}}}_i^{\mathrm{T}}\boldsymbol{M}_l^{\mathrm{T}}\boldsymbol{D}_i^{\mathrm{T}} - \hat{\boldsymbol{\mathcal{Y}}}_i^{\mathrm{T}}(\boldsymbol{M}_l^{-})^{\mathrm{T}}\boldsymbol{D}_i^{\mathrm{T}},$$
$$\hat{\boldsymbol{\mathcal{X}}}_i = \boldsymbol{K}\boldsymbol{G}_i, \hat{\boldsymbol{\mathcal{Y}}}_i = \boldsymbol{H}\boldsymbol{G}_i.$$

Here, $\boldsymbol{K}$ and $\boldsymbol{H}$ are used in the derivation to denote the controller inputs under the modal independent control strategy.

**Remark 3** The definition of an MID controller is considered as $\boldsymbol{u}(k) = \boldsymbol{K}\boldsymbol{x}(k)$. Moreover, Eq. (35) can be satisfied via Lemma 1:

$$\boldsymbol{\sigma}(\boldsymbol{K}\boldsymbol{x}(k)) = \sum_{l=1}^{2^m} \eta_l(k)(\boldsymbol{M}_l\boldsymbol{K} + \boldsymbol{M}_l^{-}\boldsymbol{H})\boldsymbol{x}(k). \quad (35)$$

As a special case, MID control is considered as a conservative control strategy. Similar to the above process, condition (34) can be obtained based on Eq. (35).

## 4 Simulations

In this section, we verify the validity of the sufficient conditions. Using the MATLAB LMI toolbox, we solve for the parameters of the MD controller. The outcomes of the simulations are then visually presented through graphical representations.

**Example 1** We consider a four-mode discrete-time MJS, whose parameters are as follows (Wang YJ et al., 2012):

$$\boldsymbol{A}_1 = \begin{bmatrix} 1.72 & -1.40 \\ 0.80 & -0.80 \end{bmatrix}, \boldsymbol{A}_2 = \begin{bmatrix} 1.58 & -0.36 \\ 0.80 & -1.12 \end{bmatrix},$$
$$\boldsymbol{A}_3 = \begin{bmatrix} 0.76 & -0.28 \\ 0.80 & -0.96 \end{bmatrix}, \boldsymbol{A}_4 = \begin{bmatrix} 1.28 & -0.38 \\ 0.80 & -0.88 \end{bmatrix},$$
$$\boldsymbol{B}_1 = \begin{bmatrix} 2 \\ 1 \end{bmatrix}, \boldsymbol{B}_2 = \begin{bmatrix} 5 \\ -6 \end{bmatrix}, \boldsymbol{B}_3 = \begin{bmatrix} 1 \\ 1 \end{bmatrix}, \boldsymbol{B}_4 = \begin{bmatrix} 0.8 \\ -1 \end{bmatrix},$$
$$\boldsymbol{C}_1 = \boldsymbol{C}_2 = \boldsymbol{C}_3 = \boldsymbol{C}_4 = \begin{bmatrix} 0.1 & 0 \end{bmatrix},$$
$$\boldsymbol{D}_1 = \boldsymbol{D}_2 = \boldsymbol{D}_3 = \boldsymbol{D}_4 = 0.2,$$
$$\boldsymbol{F}_1 = \boldsymbol{F}_2 = \boldsymbol{F}_3 = \boldsymbol{F}_4 = \begin{bmatrix} 0.1 \\ 0.1 \end{bmatrix},$$
$$\boldsymbol{\Pi} = \begin{bmatrix} 0.3 & 0.3 & 0.1 & 0.3 \\ 0.25 & 0.25 & 0.3 & 0.2 \\ 0.3 & 0.1 & 0.3 & 0.3 \\ 0.2 & 0.3 & 0.2 & 0.3 \end{bmatrix}, \boldsymbol{x}(0) = \begin{bmatrix} -2 \\ 1.5 \end{bmatrix}.$$

The external disturbance is considered as $\boldsymbol{\omega}(k) = 1/k$. It should be particularly noted that in Example 1, the system parameter matrices $\boldsymbol{D}_1$–$\boldsymbol{D}_4$ and the external disturbance $\boldsymbol{\omega}(k)$ are considered one-dimensional. Setting performance index $\gamma = 1$, we can obtain $\rho_{\min} = 0.3438$ by solving the optimal problem OP2 (Wang ZD et al., 2010; Ma and Zhang, 2012). Since $\rho_{\min} < 1$, this indicates that the initial state of the system is within the DoA-MSS, thereby guaranteeing the robustness of the system. Plugging $\rho_{\min}$, we can obtain the performance index $\gamma = 1.6935$. Moreover, we can obtain the following MD controller gain matrices:

$$\boldsymbol{K}_1 = \begin{bmatrix} -0.8608 & 0.6954 \end{bmatrix}, \boldsymbol{K}_2 = \begin{bmatrix} -0.0862 & -0.0603 \end{bmatrix},$$
$$\boldsymbol{K}_3 = \begin{bmatrix} -0.7719 & 0.5563 \end{bmatrix}, \boldsymbol{K}_4 = \begin{bmatrix} -1.1391 & 0.6846 \end{bmatrix},$$
$$\boldsymbol{H}_1 = \begin{bmatrix} -0.5318 & 0.4317 \end{bmatrix}, \boldsymbol{H}_2 = \begin{bmatrix} -0.0858 & -0.0590 \end{bmatrix},$$
$$\boldsymbol{H}_3 = \begin{bmatrix} -0.3512 & 0.3086 \end{bmatrix}, \boldsymbol{H}_4 = \begin{bmatrix} -0.5345 & 0.2241 \end{bmatrix}.$$

With $\boldsymbol{u}(k) = \boldsymbol{0}$, we simulate the open-loop system (1) under the aforementioned parameters to observe its state evolution without a controller. The entire state trajectory was recorded and visualized (Fig. 1), which clearly demonstrates the system's inherent instability in the absence of control. When implementing the proposed MD control law to form a closed-loop system that undergoes identical modal transitions, the system states exhibit rapid convergence as shown in Fig. 2. Comparative analysis with Fig. 1 confirms that the designed MD controller successfully stabilizes the system. The complete modal evolution trajectories experienced by the system under both conditions (Figs. 1 and 2) are chronologically documented in Fig. 3.

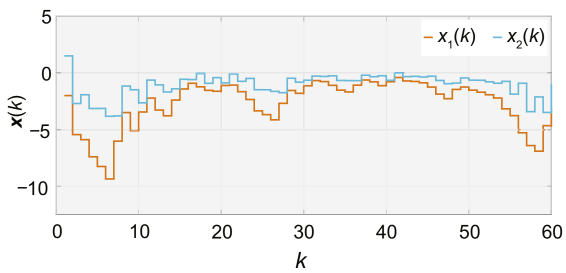


**Fig. 1 System state without controller**

**Example 2** This example uses a direct current (DC) motor device to demonstrate the superiority of our MD controller design technology. The DC motor device (Oliveira et al., 2014) can be modeled

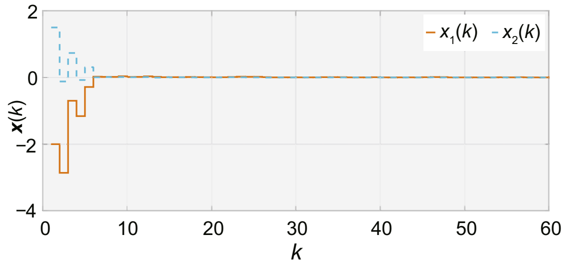


**Fig. 2 System state under the MD controller in Example 1**

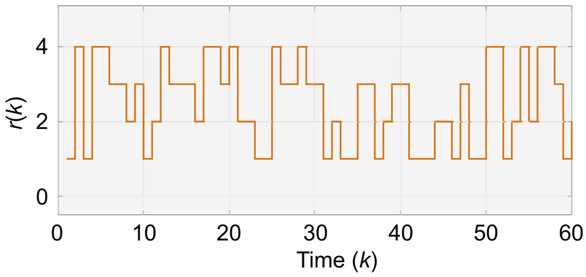


**Fig. 3 System's mode evolution**

as system (1) with the following parameters:

$$\boldsymbol{A}_1=\begin{bmatrix}-0.4799 & 5.1546 & 0\\ -3.8162 & 14.4732 & 0\\ 0.1399 & 0 & -0.9255\end{bmatrix},$$

$$\boldsymbol{A}_2=\begin{bmatrix}-1.6026 & 9.1632 & 0\\ -0.5918 & 3.0317 & 0\\ 0.0740 & 0 & -0.4338\end{bmatrix},$$

$$\boldsymbol{A}_3=\begin{bmatrix}0.6346 & 0.9178 & 0\\ -0.5056 & 2.4811 & 0\\ 0.3865 & 0 & 0.0982\end{bmatrix},$$

$$\boldsymbol{B}_1=\begin{bmatrix}5.8705\\ 15.5010\\ 0\end{bmatrix}, \boldsymbol{B}_2=\begin{bmatrix}10.2951\\ 2.2282\\ 0\end{bmatrix}, \boldsymbol{B}_3=\begin{bmatrix}0.7874\\ 1.5302\\ 0\end{bmatrix},$$

$$\boldsymbol{C}_i=\begin{bmatrix}1 & 0 & 0\\ 0 & 1.5 & 0\\ 0 & 0 & 2.5\end{bmatrix}, \boldsymbol{D}_i=\begin{bmatrix}0\\ 0\\ 0.5\end{bmatrix},$$

$$\boldsymbol{F}_i=\begin{bmatrix}0.1 & 0 & 0\\ 0 & 0.1 & 0\\ 0 & 0 & 0.1\end{bmatrix}.$$

The TPM is given as follows:

$$\boldsymbol{\Pi}=\begin{bmatrix}0.9 & 0.05 & 0.05\\ 0.36 & 0.6 & 0.04\\ 0.1 & 0.1 & 0.8\end{bmatrix}.$$

The external disturbance input is considered as follows:

$$\boldsymbol{\omega}(k)=\begin{bmatrix}v(k) & v(k) & v(k)\end{bmatrix}^{\mathrm{T}},$$

$$v(k)=\begin{cases}0.9^k\tilde{v}(k), & 0\le k\le 20,\\ -0.5, & 50\le k\le 55,\\ 0, & \text{otherwise},\end{cases}$$

where $\tilde{v}(k)$ is a random signal between −1 and 1.

Under the initial state $\boldsymbol{x}(0)=\begin{bmatrix}-5 & 3 & -2\end{bmatrix}^{\mathrm{T}}$, both the MID and MD control strategies are implemented for comparative simulation analysis. The state trajectories of the DC motor system under the same modal evolution process are recorded and presented in Figs. 4 and 5 when applying MID and MD controllers, respectively. The comparative results demonstrate that the MD control strategy achieves superior control performance compared to the MID strategy. This outcome aligns with our theoretical predictions, as the MD control paradigm effectively uses system information to enhance closed-loop stability.

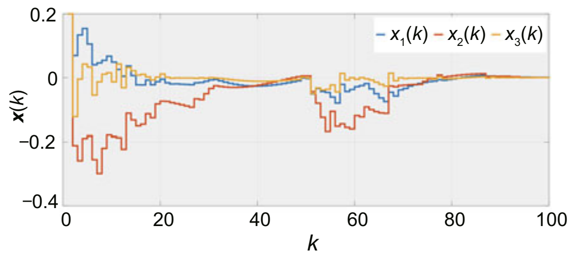


**Fig. 4 System state under the MID controller in Example 2**

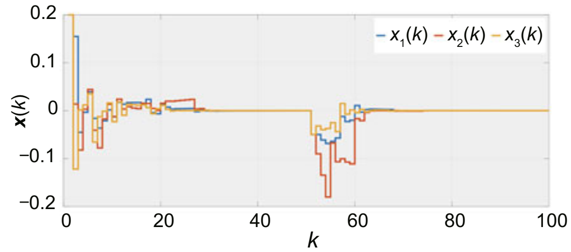


**Fig. 5 System state under the MD controller in Example 2**

## 5 Conclusions

An MD controller design methodology has been proposed to guarantee the mean-square stability and stochastic passivity for discrete-time MJSs with actuator saturation. By introducing a saturation-dependent Lyapunov function, we have derived relatively less conservative sufficient conditions. An MID control corollary has been introduced as a special case to complement our theoretical findings. At the end of this paper, the superiority of our theoretical result has been validated through two numerical examples. Notably, with the advancement of communication network technologies, engineering requirements for networked system stability, and the security have become increasingly stringent. In scenarios involving unobservable mode information and constrained network bandwidth resources, we will further investigate robust control strategies under denial-of-service (DOS) attacks using asynchronous event-triggered control mechanisms, and we think it is a challenging research direction.

## Contributors

Liqing WANG guided the research. Jiaming TANG designed the research and drafted the paper. Mingkun WANG and Feiyu YANG conducted and analyzed the simulations. All the authors participated in writing the paper. Mingkun WANG revised the paper, and Liqing WANG finalized the paper.

## Conflict of interest

All the authors declare that they have no conflict of interest.

## Data availability

The data that support the findings of this study are available from the corresponding author upon reasonable request.

## References


Bolzern P, Colaneri P, De Nicolao G, 2014. Stochastic stability of positive Markov jump linear systems. *Automatica*, 50(4):1181-1187. https://doi.org/10.1016/j.automatica.2014.02.016

Cao YY, Lin ZL, Shamash Y, 2002. Set invariance analysis and gain-scheduling control for LPV systems subject to actuator saturation. *Syst Contr Lett*, 46(2):137-151. https://doi.org/10.1016/S0167-6911(02)00128-7

Chen GL, Sun J, Chen J, 2020. Passivity-based robust sampled-data control for Markovian jump systems. *IEEE Trans Syst Man Cybern Syst*, 50(7):2671-2684. https://doi.org/10.1109/TSMC.2018.2825474

Chen GL, Fan CC, Sun J, et al., 2022a. Mean square exponential stability analysis for Itô stochastic systems with aperiodic sampling and multiple time-delays. *J. IEEE Trans Autom Contr*, 67(5):2473-2480. https://doi.org/10.1109/TAC.2021.3074848

Chen GL, Xia JW, Park JH, et al., 2022b. Sampled-data synchronization of stochastic Markovian jump neural networks with time-varying delay. *IEEE Trans Neur Netw Learn Syst*, 33(8):3829-3841. https://doi.org/10.1109/TNNLS.2021.3054615

Chen GL, Du GX, Xia JW, et al., 2023. Controller synthesis of aperiodic sampled-data networked control system with application to interleaved flyback module integrated converter. *IEEE Trans Circ Syst I Regul Pap*, 70(11):4570-4580. https://doi.org/10.1109/TCSI.2023.3295940

Chen GL, Du GX, Xia JW, et al., 2024. Aperiodic sampled-data $H_\infty$ control of vehicle active suspension system: an uncertain discrete-time model approach. *IEEE Trans Ind Inform*, 20(4):6739-6750. https://doi.org/10.1109/TII.2024.3353856

Cheng P, Wang JC, He SP, et al., 2020. Observer-based asynchronous fault detection for conic-type nonlinear jumping systems and its application to separately excited DC motor. *IEEE Trans Circ Syst I Regul Pap*, 67(3):951-962. https://doi.org/10.1109/TCSI.2019.2949368

Cheng P, He SP, Cheng J, et al., 2021. Asynchronous output feedback control for a class of conic-type nonlinear hidden Markov jump systems within a finite-time interval. *IEEE Trans Syst Man Cybern Syst*, 51(12):7644-7651. https://doi.org/10.1109/TSMC.2020.2980312

Costa OLV, Marques RP, Fragoso MD, 2005. Discrete-Time Markov Jump Linear Systems. Springer London, UK. https://doi.org/10.1007/b138575

Feng ZG, Shi P, 2017. Sliding mode control of singular stochastic Markov jump systems. *IEEE Trans Autom Contr*, 62(8):4266-4273. https://doi.org/10.1109/TAC.2017.2687048

Goncalves APC, Fioravanti AR, Geromel JC, 2009. $\mathcal{H}_\infty$ filtering of discrete-time Markov jump linear systems through linear matrix inequalities. *IEEE Trans Autom Contr*, 54(6):1347-1351. https://doi.org/10.1109/TAC.2009.2015553

Hu TS, Lin ZL, 2001. Control Systems with Actuator Saturation. Birkhäuser Boston MA, USA. https://doi.org/10.1007/978-1-4612-0205-9

Jiang YH, Wu W, Lou XY, et al., 2021. Event-based $H_\infty$ control for piecewise-affine systems subject to actuator saturation. *Front Inform Technol Electron Eng*, 22(5):720-731. https://doi.org/10.1631/FITEE.1900601

Liu HP, Sun FC, Boukas EK, 2006. Robust control of uncertain discrete-time Markovian jump systems with actuator saturation. *Int J Contr*, 79(7):805-812. https://doi.org/10.1080/00207170600688842

Ma SP, Zhang CH, 2012. $H_\infty$ control for discrete-time singular Markov jump systems subject to actuator saturation. *J Franklin Inst*, 349(3):1011-1029. https://doi.org/10.1016/j.jfranklin.2011.12.004

Nie R, Du WL, Li ZM, et al., 2024. Finite-time consensus control for MASs under hidden Markov model mechanism. *IEEE Trans Autom Contr*, 69(7):4726-4733. https://doi.org/10.1109/TAC.2024.3351947

Oliveira RCLF, Vargas AN, do Val JBR, et al., 2014. Mode-independent $\mathcal{H}_2$-control of a DC motor modeled as a Markov jump linear system. *IEEE Trans Contr Syst*

*Technol*, 22(5):1915-1919.
https://doi.org/10.1109/TCST.2013.2293627

Pang Z, Wang H, Cheng J, et al., 2024. Stability and fuzzy optimal control for nonlinear Itô stochastic Markov jump systems via hybrid reinforcement learning. *IEEE Trans Fuzzy Syst*, 32(11):6472-6485.
https://doi.org/10.1109/TFUZZ.2024.3450912

Tao YY, Wu ZG, 2024. Asynchronous static output-feedback control of Markovian jump linear systems. *IEEE Trans Autom Contr*, 69(4):2453-2460.
https://doi.org/10.1109/TAC.2023.3305345

Wang S, Wu ZG, 2022. Asynchronous control of uncertain Markov jump systems with actuator saturation. *IEEE Trans Circ Syst II Express Briefs*, 69(7):3269-3273.
https://doi.org/10.1109/TCSII.2022.3158726

Wang S, Wu ZG, 2024. Asynchronous energy-to-peak filtering for restricted Markov jump systems. *IEEE Trans Autom Contr*, 69(5):2823-2838.
https://doi.org/10.1109/TAC.2023.3293019

Wang S, Wu ZG, Tao YY, 2023. Asynchronous $H_\infty$ control for continuous-time hidden Markov jump systems with actuator saturation. *IEEE Trans Cybern*, 53(11):7095-7104. https://doi.org/10.1109/TCYB.2022.3181820

Wang YJ, Sun YN, Zuo ZQ, et al., 2012. Robust $H_\infty$ control of discrete-time Markovian jump systems in the presence of incomplete knowledge of transition probabilities and saturating actuator. *Int J Robust Nonl Contr*, 22(15):1753-1764.
https://doi.org/10.1002/rnc.1783

Wang ZD, Ho DWC, Dong HL, et al., 2010. Robust $\mathcal{H}_\infty$ finite-horizon control for a class of stochastic nonlinear time-varying systems subject to sensor and actuator saturations. *IEEE Trans Autom Contr*, 55(7):1716-1722. https://doi.org/10.1109/TAC.2010.2047033

Wu YY, Cheng J, Zhou X, et al., 2021. Asynchronous filtering for nonhomogeneous Markov jumping systems with deception attacks. *Appl Math Comput*, 394:125790.
https://doi.org/10.1016/j.amc.2020.125790

Wu ZG, Shi P, Su HY, et al., 2014. Asynchronous filtering for discrete-time stochastic Markov jump systems with randomly occurred sensor nonlinearities. *Automatica*, 50(1):180-186.
https://doi.org/10.1016/j.automatica.2013.09.041

Wu ZG, Shi P, Shu Z, et al., 2017. Passivity-based asynchronous control for Markov jump systems. *IEEE Trans Autom Contr*, 62(4):2020-2025.
https://doi.org/10.1109/TAC.2016.2593742

Xu TS, Niu YG, Cao ZR, 2024. Attack-tolerant control for Markovian jump systems with stochastic sampling: a sliding mode scheme. *Automatica*, 161:111496.
https://doi.org/10.1016/j.automatica.2023.111496

Xu Y, Wu ZG, Sun J, 2023. Security-based passivity analysis of Markov jump systems via asynchronous triggering control. *IEEE Trans Cybern*, 53(1):151-160.
https://doi.org/10.1109/TCYB.2021.3090398

Zhang M, Shi P, Liu ZT, et al., 2018. Dissipativity-based asynchronous control of discrete-time Markov jump systems with mixed time delays. *Int J Robust Nonl Contr*, 28(6):2161-2171.
https://doi.org/10.1002/rnc.4005

Zhao XD, Zhang LX, Shi P, et al., 2012. Stability and stabilization of switched linear systems with mode-dependent average dwell time. *IEEE Trans Autom Contr*, 57(7):1809-1815.
https://doi.org/10.1109/TAC.2011.2178629